Beam observations towards Mars

Version 1.1 of 2010-11-17, by Michael Olberg

Abstract

Note on results from beam measurements on Mars during HIFI PSP and Routine Phase.

Technical Note: ICC/2010-nnn

11 pages

Introduction

A series of beam measurements towards Mars were performed during ODs 330 and 331, all employing the engineering mode `HifiMappingProcFastDBSRaster` with a 7×7 raster at half beam spacing. One frequency per LO subband was observed, with the exception of band 7b where two frequencies were used. A second series of beam measurements towards Mars at a subset of these frequencies were performed during ODs 390, 391, 406 and 407. Table 1 lists the observations.

	OD	ObsID	band	freq
1	331	1342194179	1a	491
2	330	1342194154	1b	610
3	330	1342194152	2a	648
4	330	1342194150	2b	770
5	330	1342194148	3a	828
6	331	1342194165	3b	948
7	330	1342194146	4a	1012
8	331	1342194167	4b	1112
9	330	1342194144	5a	1127
10	331	1342194169	5b	1243
11	331	1342194171	6a	1483
12	331	1342194175	6b	1625
13	331	1342194173	7a	1703
14	330	1342194156	7b	1807
15	330	1342194157	7b	1893
16	390	1342197929	1b	610
17	406	1342199101	2b	770
18	390	1342197931	3b	948
19	391	1342197950	4a	1012
20	407	1342199664	5a	1127
21	407	1342199666	5b	1243
22	406	1342199105	6b	1625
23	390	1342197940	7b	1807
24	407	1342199674	7b	1893

Table 1: List of Mars observations

Fitting of 2-D Gaussian profiles

We start by fitting circular symmetric Gaussian distributions to the observed intensity distributions of integrated intensities, i.e we fit a function:

$$I(x,y) = I_0 \cdot \exp\left[-4\ln 2\left(\left(\frac{x-x_0}{\theta_{obs}}\right)^2 + \left(\frac{y-y_0}{\theta_{obs}}\right)^2\right)\right]$$

with amplitude I_0, center position (x_0, y_0) and full width at half maximum (FWHM) in both axes θ_{obs}. The achieved positions have been analyzed in terms of pointing performance elsewhere, here we focus on the fitted amplitudes and widths[1]

Beam widths

In order to compare the observed beam widths with theoretical expectations we need to deconvolve the contribution from the Mars disk from the observed FWHMs (θ_{obs}). We do this by using the following formula:

$$\theta_b = \sqrt{\theta_{obs}^2 - a \cdot \theta_s^2}$$

where $\theta_s \approx 8.5$ (5.5) arcsec is the apparent diameter of Mars at the time of the first (second) set of observations. The factor a describes the expected beam broadening resulting from the convolution of the beam with the Mars disk. For the case of a 2-dimensional Gaussian convolved with a circular disk of constant brightness this can be calculated to be $a = \frac{\ln 2}{2}$ for disk diameters smaller than (half) the beam size. This factor was also verified by numerically convolving 2-dimensional Gaussian beams with model surface brightness distributions for Mars and was found to be close ($\pm 5\%$) to the theoretical value for both sets of observations.
For the Herschel telescope with an effective diameter of $D_{eff} = 3.28\,\mathrm{m}$, the expected HPBW θ_b is given as a function of the wavelength and the telescope diameter D (see [1], Eqs. 6.40 and 6.41)

$$\theta_b = \frac{2}{\pi}\left(1.6 + 0.021 \cdot T_e(\mathrm{dB})\right) \cdot \frac{\lambda}{D} \qquad (1)$$

This relation between HPBW and wavelength is a straight line through the origin, which we can use in order to fit the data and derive the edge taper T_e. Note, however that according to Eq. 1 the edge taper only mildly affects the HPBW and therefore will not be constrained very tightly by a linear fit.
Figure 1 shows the result. The data are fitted by an edge taper of $T_e = 7.94\,\mathrm{dB}$ with a 95% confidence interval of $\Delta T_e = \pm 0.82\,\mathrm{dB}$. This is to be compared with the designed edge taper (for the unobstructed aperture) of 10.9 dB. It is worth noting that the beam widths observed during the second run are systematically lower than the first run. This behavior

[1]Data reduction was performed with HIPE version 4.0.x, when the task `doAntennaTemperature` was using a forward efficiency of 1.0, therefore effectively not performing the translation from $T_A' \rightarrow T_A^*$.

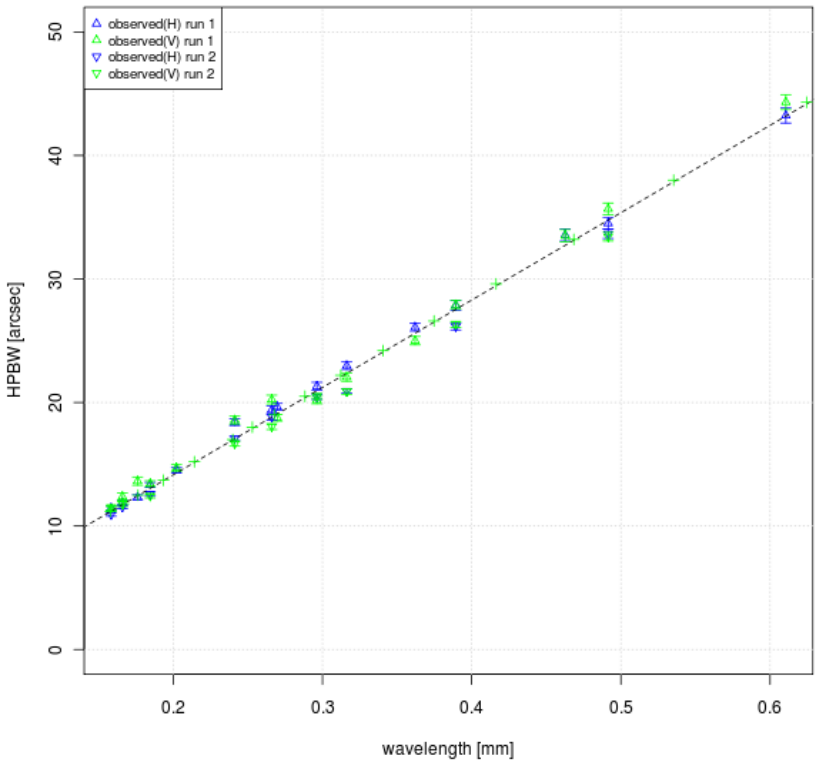

Figure 1: Observed and fitted beam widths, error bars are given by errors of the fitted observed beam widths.

will be analyzed further. However, the fit over all data agrees very well with calculations of expected beam widths done by Willem Jellema.

Beam efficiencies

For the coupling of a Gaussian beam to a disklike source of diameter θ_s we calculate:

$$x = \sqrt{\ln 2}\,\frac{\theta_s}{\theta_b}$$

$$F_d = \frac{1}{1 - \mathrm{e}^{-x^2}}$$

and using this coupling we can transform predicted Rayleigh Jeans temperatures T_{RJ} for Mars[2] into antenna temperatures

[2] `http://www.lesia.obspm.fr/perso/emmanuel-lellouch/mars/`

$$T'_A = \eta_{mb} \frac{T_{RJ}}{F_d} \tag{2}$$

The main beam efficiency η_{mb} is expected to vary with wavelength according to Ruze's formula:

$$\eta_{mb} = \eta_{mb,0} \cdot \exp\left[-\left(\frac{4\pi\sigma}{\lambda}\right)^2\right] \tag{3}$$

where σ is the surface accuracy of the Herschel telescope of 3 µm.
We fit the linear relation (Eq. 2) between Rayleigh-Jeans temperatures (multiplied by the exponential describing the dependence on the surface roughness and divided by the coupling to the Mars disk) and the observed antenna temperatures in order to derive the factor $\eta_{mb,0}$ that best fits the data.[3]

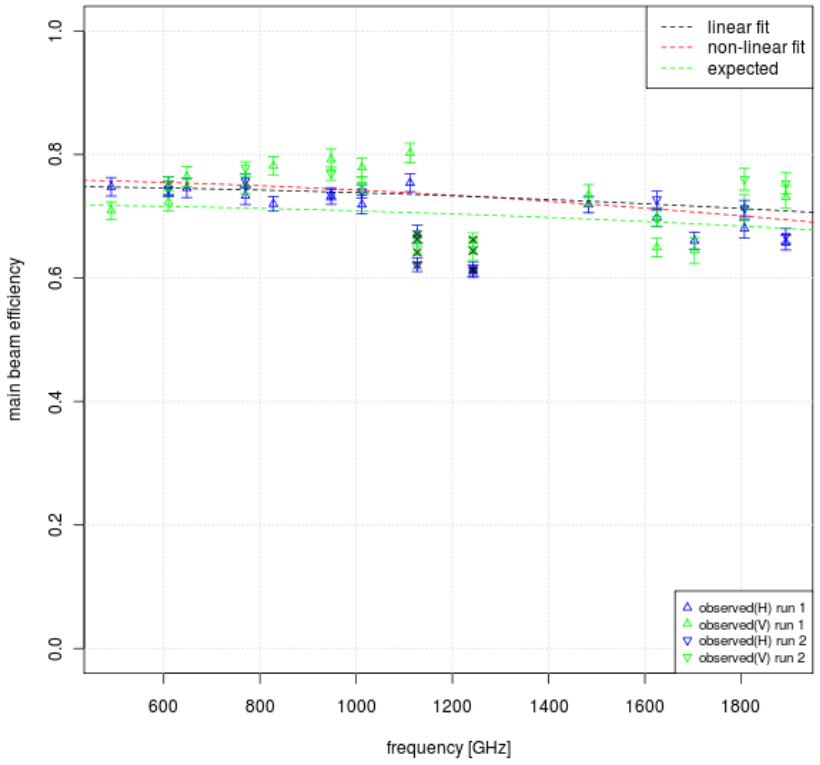

Figure 2: Observed main beam efficiencies as a function of frequency. Error bars are based on errors of fitted beam widths and amplitudes of the Mars observations, uncertainties in the Mars model are not included. Band 5 observations are marked with black crosses.

[3]For the time being we exclude from our fit observations in band 5, which show systematically lower values.

For the data from both run 1 and 2 a linear fit yields $\eta_{mb,0} = 0.75$ for a fixed surface error of 3 µm. Fitting both $\eta_{mb,0}$ and σ in a non-linear fit yields $\eta_{mb,0} = 0.76$ and $\sigma = 3.8$ µm. Expected pre-flight values were $\eta_{mb,0} = 0.72$ and $\sigma = 3$ µm (see [2]).

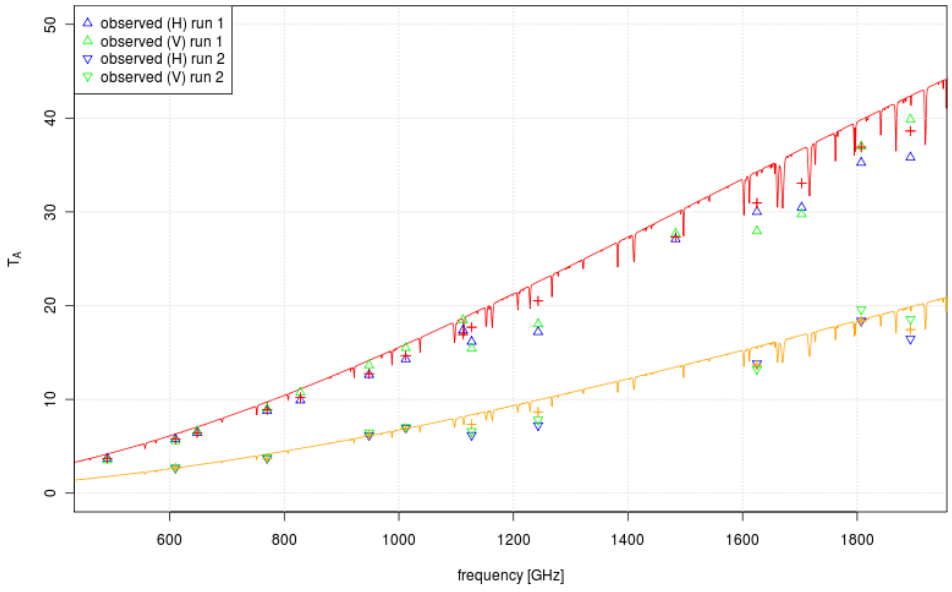

Figure 3: Predicted and observed antenna temperatures using the fitted efficiencies and HPBWs from the previous sections. The prediction based on the Mars model made available to the HCalSG by R. Moreno is shown by the red (orange) line, the more precise values from the above mentioned web-site which were used for the fit are shown as red (orange) plus signs. Observed antenna temperatures are shown by open triangles, color coded according to polarization.

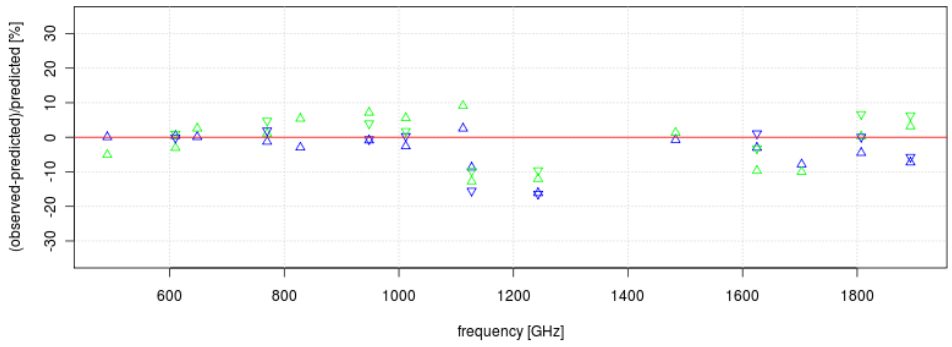

Figure 4: Relative deviations between observed and predicted antenna temperatures.

Aperture efficiencies

Alternatively, we can use the procedure outlined in [2] to derive aperture efficiencies from our measurements. Given the frequency ν of the observation, the HPBW θ_b at this frequency, the diameter of the (disk like) source θ_s and its brightness temperature at the observing frequency, the expected antenna temperature is calculated as:

$$T'_{\rm A} = \frac{S_{\nu,tot} A_{\rm eff}}{2k} K$$

with correction factor

$$K = \frac{1-\exp(-x^2)}{x^2} \leq 1$$

where

$$x = \sqrt{\ln 2}\ \ \frac{\theta_s}{\theta_b}$$

The effective antenna area $A_{\rm eff}$ is related to the true, geometrical area of the antenna $A_{\rm geom} = \pi\frac{D^2}{4}$ via the wanted aperture efficiency $A_{\rm eff} = \eta_A A_{\rm geom}$. Here we use $D = 3.28\,{\rm m}$ as the effective diameter of the Herschel telescope (see [2]).
The total flux $S_{\nu,tot}$ is calculated as

$$S_{\nu,tot} = \frac{2k\nu^2}{c^2}\frac{\pi}{4}\theta_s^2 J_\nu(T_B)$$

with $J_\nu(T_B)$ being the Rayleigh-Jeans brightness temperature at the frequency ν:

$$J_\nu(T_B) \equiv T_{RJ} = \frac{h\nu}{k}\frac{1}{\exp(\frac{h\nu}{kT_B})-1}$$

The results are plotted in Fig 5 together with a non-linear fit[4] (of parameters $\eta_{A,0}$ and σ) to the relation

$$\eta_A = \eta_{A,0}\cdot\exp\left[-\left(\frac{4\pi\sigma}{\lambda}\right)^2\right] \tag{4}$$

We find $\eta_{A,0} = 0.68$ and a surface error rms of $\sigma = 3.8\,\mu{\rm m}$. The graph also shows a prediction based on the expected values $\eta_{A,0} = 0.71$ and $\sigma = 3\,\mu{\rm m}$. Fitting only $\eta_{A,0}$, but keeping the surface error of $3\,\mu{\rm m}$, yields a value of 0.67. The ratio between our derived $\eta_{mb,0}$ and $\eta_{A,0}$ is 1.108 (non-linear fit) or 1.126 (linear fit), to be compared with the expected 1.015. Note, that for the aperture efficiencies the observed values are lower than expectations based on [2], whereas observed main beam efficiencies were slightly larger than pre-flight expectations.
We can transform the observed aperture efficiencies into main beam efficiencies via

$$\frac{\eta_{mb}}{\eta_A} = \frac{A_{geom}\Omega_{mb}}{\lambda^2} \approx \frac{\pi D^2}{4}\frac{\pi}{4\ln 2}\frac{\theta_b^2}{\lambda^2}$$

The results are, however, indistinguishable from what is shown in Fig 2 and therefore not reproduced here.

[4]Band 5 measurements are again excluded.

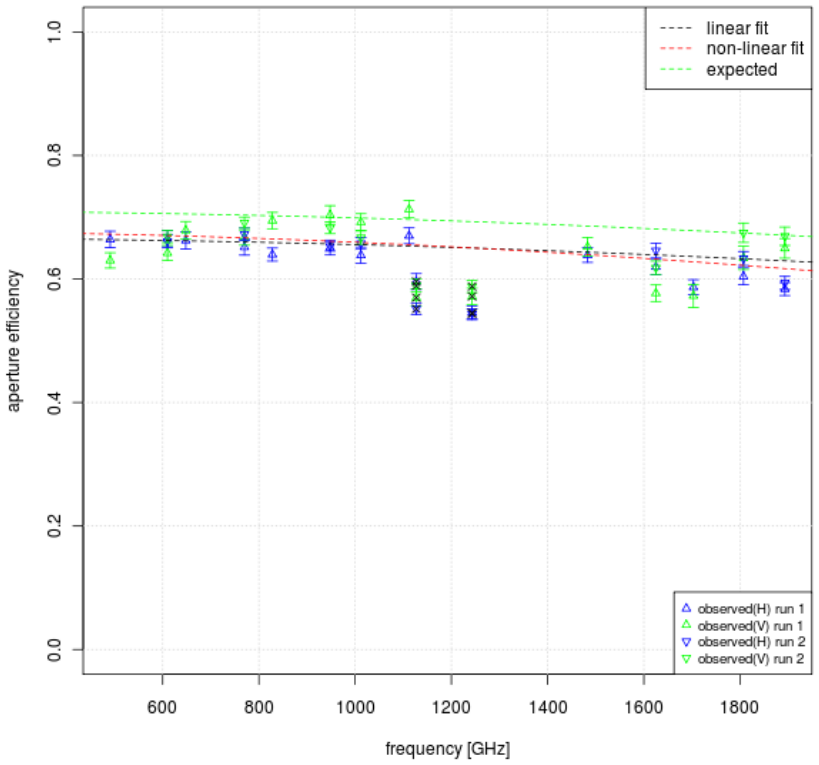

Figure 5: Fitted aperture efficiencies, compared to expected values based on $\eta_{A,0} = 0.71$. Band 5 observations are marked with black crosses.

Recommendation

Table 2: Recommended efficiencies. Errors quoted are 95% confidence intervals.

bands	$\eta_{mb,0}$	$\eta_{A,0}$	σ [µm]	comment
1–4,6–7	0.76 ± 0.02	0.68 ± 0.02	3.8 ± 0.9	non-linear fit
5	0.66 ± 0.02	0.58 ± 0.02	3.8 ± 0.9	average

For the moment the HIFI ICC advises to use the values for $\eta_{mb,0}$ or $\eta_{A,0}$ as well as the surface accuracy σ given in Table 2 for the band in question, and calculate the required main beam or aperture efficiency at any given frequency within that band by applying equation 3 or 4, respectively.

References

[1] Goldsmith, P. F., 1998: *Quasioptical Systems*

[2] Kramer, C., 2006: *Spatial response framework document*

Table 3: Results for (**H**). Columns 4–6 show disk diameter, brightness and Rayleigh-Jeans temperature from the Mars model. Columns 7–8 show calculated main beam temperatures and total flux. Column 9 is the observed antenna temperature and, finally, columns 10–11 show the resulting efficiencies.

run	ν	θ_b	θ_s	T_b	T_{RJ}	T_{mb}	$S_{\nu,tot}$	T'_A	η_{mb}	η_A
	GHz	arcsec	arcsec	K	K	K	Jy	K		
1	491	43.2	8.475	199.6	188.048	4.953	1846.8	3.703	0.748	0.664
1	610	34.5	8.569	201.3	187.041	7.715	2898.5	5.776	0.749	0.665
2	610	33.7	5.774	204.7	190.410	3.607	1339.7	2.685	0.744	0.661
1	648	33.6	8.572	201.2	186.046	8.642	3255.7	6.445	0.746	0.662
1	770	27.8	8.576	202.1	184.192	11.975	4555.5	8.783	0.733	0.652
2	770	26.1	5.356	207.8	189.898	4.915	1831.9	3.721	0.757	0.673
1	828	26.1	8.580	202.9	183.717	13.753	5258.9	9.902	0.720	0.640
1	948	23.0	8.531	201.4	179.555	17.222	6660.8	12.619	0.733	0.651
2	948	20.9	5.772	207.9	186.018	8.391	3158.9	6.168	0.735	0.653
1	1012	21.3	8.584	204.4	181.039	19.883	7748.6	14.292	0.719	0.639
2	1012	20.5	5.754	207.2	183.906	9.367	3536.8	6.935	0.740	0.658
1	1112	19.6	8.526	203.3	177.819	23.010	9065.5	17.353	0.754	0.670
1	1127	19.4	8.588	204.9	179.063	24.079	9513.7	16.152	0.671	0.596
2	1127	18.8	5.346	209.0	183.100	9.965	3769.7	6.189	0.621	0.552
1	1243	18.4	8.522	204.7	176.348	28.013	11223.0	17.193	0.614	0.545
2	1243	17.1	5.342	208.1	179.744	11.812	4494.9	7.228	0.612	0.544
1	1483	14.5	8.515	206.5	172.932	37.690	15640.1	27.099	0.719	0.639
1	1625	13.3	8.495	205.5	169.011	43.023	18266.7	30.006	0.697	0.620
2	1625	12.6	5.352	209.2	172.620	18.999	7405.3	13.815	0.727	0.646
1	1703	12.3	8.504	205.2	167.049	46.151	19871.5	30.476	0.660	0.587
1	1807	11.9	8.562	208.3	167.920	51.818	22797.2	35.245	0.680	0.604
2	1807	11.5	5.762	207.8	167.479	25.776	10297.6	18.373	0.713	0.633
1	1893	11.4	8.552	206.1	163.986	54.506	24375.6	35.817	0.657	0.584
2	1893	10.9	5.338	211.2	168.995	24.614	9786.9	16.447	0.668	0.594

Table 4: Same as Table 3 for (**V**).

run	ν	θ_b	θ_s	T_b	T_{RJ}	T_{mb}	$S_{\nu,tot}$	T'_A	η_{mb}	η_A
	GHz	arcsec	arcsec	K	K	K	Jy	K		
1	491	44.3	8.475	199.6	188.048	4.953	1846.8	3.513	0.709	0.630
1	610	35.7	8.569	201.3	187.041	7.715	2898.5	5.576	0.723	0.642
2	610	33.4	5.774	204.7	190.410	3.607	1339.7	2.715	0.753	0.669
1	648	33.5	8.572	201.2	186.046	8.642	3255.7	6.603	0.764	0.679
1	770	27.9	8.576	202.1	184.192	11.975	4555.5	8.992	0.751	0.667
2	770	26.3	5.356	207.8	189.898	4.915	1831.9	3.824	0.778	0.691
1	828	25.0	8.580	202.9	183.717	13.753	5258.9	10.753	0.782	0.695
1	948	22.1	8.531	201.4	179.555	17.222	6660.8	13.642	0.792	0.704
2	948	20.9	5.772	207.9	186.018	8.391	3158.9	6.451	0.769	0.683
1	1012	20.2	8.584	204.4	181.039	19.883	7748.6	15.492	0.779	0.692
2	1012	20.5	5.754	207.2	183.906	9.367	3536.8	7.034	0.751	0.667
1	1112	18.8	8.526	203.3	177.819	23.010	9065.5	18.466	0.803	0.713
1	1127	20.2	8.588	204.9	179.063	24.079	9513.7	15.442	0.641	0.570
2	1127	18.0	5.346	209.0	183.100	9.965	3769.7	6.610	0.663	0.589
1	1243	18.6	8.522	204.7	176.348	28.013	11223.0	18.032	0.644	0.572
2	1243	16.7	5.342	208.1	179.744	11.812	4494.9	7.816	0.662	0.588
1	1483	14.7	8.515	206.5	172.932	37.690	15640.1	27.664	0.734	0.652
1	1625	13.4	8.495	205.5	169.011	43.023	18266.7	27.943	0.649	0.577
2	1625	12.4	5.352	209.2	172.620	18.999	7405.3	13.223	0.696	0.618
1	1703	13.6	8.504	205.2	167.049	46.151	19871.5	29.754	0.645	0.573
1	1807	12.4	8.562	208.3	167.920	51.818	22797.2	36.989	0.714	0.634
2	1807	11.8	5.762	207.8	167.479	25.776	10297.6	19.585	0.760	0.675
1	1893	11.4	8.552	206.1	163.986	54.506	24375.6	39.858	0.731	0.650
2	1893	11.5	5.338	211.2	168.995	24.614	9786.9	18.544	0.753	0.669